

Map of Two-Dimensional Tungsten Chalcogenide Compounds (W–S, W–Se, W–Te) Based on USPEX Evolutionary Search

E. V. Sukhanova^a, A. G. Kvashnin^{b, a}, M. A. Agamalyan^c, H. A. Zakaryan^c, and Z. I. Popov^{a, *}

^a Emanuel Institute of Biochemical Physics, Russian Academy of Sciences, Moscow, 119334 Russia

^b Skolkovo Institute of Science and Technology, Moscow, 121205 Russia

^c Yerevan State University, Yerevan, 0025 Armenia

*e-mail: zipcool@bk.ru

Received February 10, 2022; revised February 10, 2022; accepted February 11, 2022

New two-dimensional nanostructures of W–X composition (X = S, Se, Te) are predicted using the evolutionary algorithm implemented in the USPEX software package. Based on the results, two new thermodynamically and dynamically stable two-dimensional W_3S_5 and W_5Te_2 structures are proposed. The density functional theory study of the electronic and optical properties of these monolayers is carried out. It is demonstrated that the predicted W_3S_5 and W_5Te_2 structures show semiconducting properties with band gaps of 0.62 and 0.40 eV, respectively, and the calculated extinction spectrum indicates a broad absorption band in the visible spectral range, making these materials promising for applications in photovoltaics and solar energy.

DOI: 10.1134/S0021364022100162

1. INTRODUCTION

To search for new promising nanomaterials for optoelectronics, spintronics, and nanoelectronics, researchers studied in detail the monolayer properties of transition metal dichalcogenides [1–3] and various heterostructures based on them [4–6]. In particular, tungsten dichalcogenides, which exhibit a number of interesting physical and chemical properties, are of special interest. They are characterized by a strong spin–orbit interaction [7], which makes them promising for use in spintronics and valleytronics [8], and also have unique optical properties, for example, strongly bound excitons [9, 10] and the highest photoluminescence quantum yield among all two-dimensional semiconductors [11].

Like many other transition metal dichalcogenides, tungsten dichalcogenide monolayers can exist in several allotropic modifications, which are the hexagonal H phase, where tungsten atoms are in a trigonal-prismatic coordination environment of sulfur atoms, as well as the tetragonal T and T' (or Td) phases, where the tungsten atoms are in an octahedral environment [12]. Tungsten disulfide and diselenide monolayers in the ground state exist in the hexagonal H phase, in contrast to tungsten ditelluride, for which the ground state is the T' phase. H-WS₂ and H-WSe₂ are direct-gap semiconductors with a band gap of ~2 eV [7, 13]. Although the T phases of tungsten disulfide and diselenide are not energetically favorable, they can be obtained experimentally, for example, as interfaces [14, 15], grown by chemical vapor deposition [16], or

by post-processing the samples [17, 18]. In contrast, the T'-WTe₂ monolayer is a semimetal and a topological insulator [19], exhibits the spin quantum Hall effect [20], and shows superconductivity and anisotropic magnetoresistance [21]. Earlier, another hexagonal phase, H', was theoretically proposed, which can occur as an interface in two-dimensional crystals [22]. In addition to hexagonal phases, the existence of other two-dimensional compounds of WX₂ composition (X = S, Se, Te), for example, with a square lattice [23, 24] (S-WX₂), was theoretically predicted. The theoretical studies prove the dynamic stability of the predicted structures and demonstrate that such monolayers are also topological insulators [23, 24]. Moreover, the authors of [25] theoretically predicted several new dynamically stable two-dimensional transition metal dichalcogenide phases of MS₂ stoichiometry (M = Mo, W, Re).

A change in the stoichiometry of two-dimensional nanomaterials can lead to the appearance of structures with new properties [26]. For example, under certain conditions, violation of stoichiometry can occur during sample synthesis [27, 28]. In addition, such a change can be both spontaneous, under the influence of the environment [29], and controlled, for example, under the influence of irradiation with high-energy ions [30, 31] or electrons [32, 33]. The possibility of obtaining monolayers of nonstoichiometric composition, W₂S₃, was experimentally demonstrated in [32]. A theoretical study of the stability and properties of M₂X₃ monolayers (M = Mo, W; X = S, Se, Te)

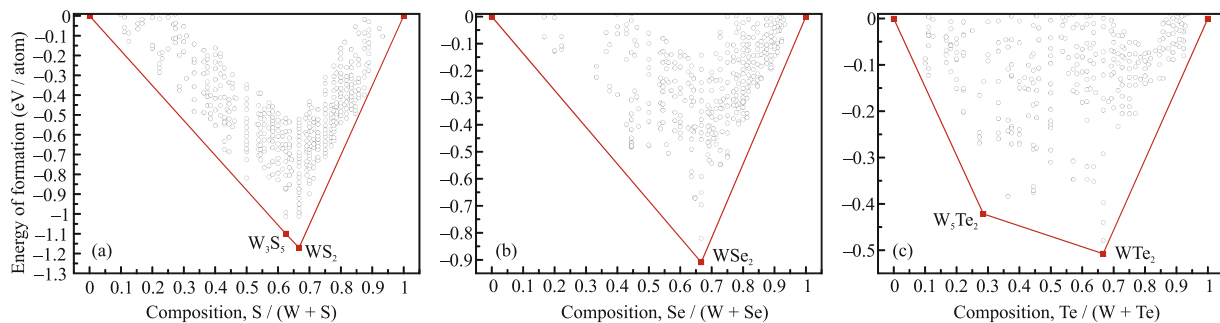


Fig. 1. (Color online) Calculated phase diagrams in the composition–formation energy coordinates for (a) W–S, (b) W–Se, and (c) W–Te systems.

demonstrated that sulfides and selenides exhibit semiconducting properties, while tellurides exhibit metallic properties; moreover, among the studied structures, only W_2Te_3 is not dynamically stable. Note that no comprehensive theoretical studies were carried out previously on the search for stable two-dimensional materials in the W–X systems ($X = \text{S}, \text{Se}, \text{Te}$) with use of global optimization methods.

In this work, the atomic structures of new two-dimensional monolayers in the W–S, W–Se, and W–Te systems are theoretically predicted using the USPEX evolutionary algorithm, and the electronic and optical properties of the predicted nanostructures are studied within the density functional theory.

2. RESEARCH METHODS

Thermodynamically stable two-dimensional structures were searched by using a combination of the USPEX evolutionary crystal structure prediction algorithm [34–36] with the density functional theory, which was used to calculate the total energy of candidate structures during the search process. The first generation of structures for evolutionary search consisted of 120 structures and was generated by arbitrary symmetry [37] and topology [38] operators. Subsequent generations (120 structures) consisted of 20% arbitrary structures, 40% structures generated by the heredity operator, 20% structures generated by the soft mode mutation operator, and 20% structures generated by the transmutation operator. During the search, the number of atoms in the unit cell of the generated structures varies from 8 to 16. Structures with a thickness up to 6 Å, which corresponds to the doubled W–Te bond length, were considered.

The relaxation of the structures was carried out within the density functional theory (DFT) [39, 40] using the generalized gradient approximation (GGA) in the Perdew–Burke–Ernzerhof (PBE) parametrization for the exchange-correlation functional [41]. The calculations were carried out in the VASP package [42–44]. The electron configurations $6s^25d^4$, $5s^25p^4$,

$3s^23p^4$, and $4s^24p^4$ were considered in the calculations for tungsten, tellurium, sulfur, and selenium atoms, respectively. The cutoff energy for the plane wave basis was set to 500 eV. The sampling of the first Brillouin zone into a k -point grid was carried out using the Monkhorst–Pack method [45] with a resolution of $2\pi \times 0.04 \text{ \AA}^{-1}$. The vacuum gap, i.e., the distance between periodically arranged layers of the structures, was no less than 15 Å, which excludes the artificial interaction between periodic images in a nonperiodic direction. Vibrational characteristics were calculated using the finite displacement method (VASP and PHONOPY [46, 47]). To accurately describe phonons in two-dimensional systems, translational and rotational invariants were taken into account [48, 49] by using the Hiphive program [50].

The optical properties were calculated using a superposition of Lorentz oscillators. The real part of the complex dielectric function was determined by means of the Kramers–Kronig relation, and the imaginary part was found by summing over unfilled states [51].

3. RESULTS

The results of the evolutionary search for stable two-dimensional compounds in the W–S, W–Se, and W–Te systems are demonstrated in Fig. 1. Note that, since WX_2 monolayers are well studied, their stability and properties are not discussed in this work.

In the W–S system, two thermodynamically stable structures with the W_3S_5 and WS_2 compositions were predicted. The WS_2 structure corresponds to the known H- WS_2 phase and is well studied both experimentally [7] and theoretically [13, 52]. The energies of the known T- and T'- WS_2 phases are slightly higher than the energy of the H phase ($\Delta E_{\text{H-T}} = 0.30 \text{ eV/atom}$ and $\Delta E_{\text{H-T'}} = 0.18 \text{ eV/atom}$); these phases are metastable and are located above the convex hull (see Fig. 1a). In the W–Se system, in addition to pure substances, only the known structure of the WSe_2 mono-

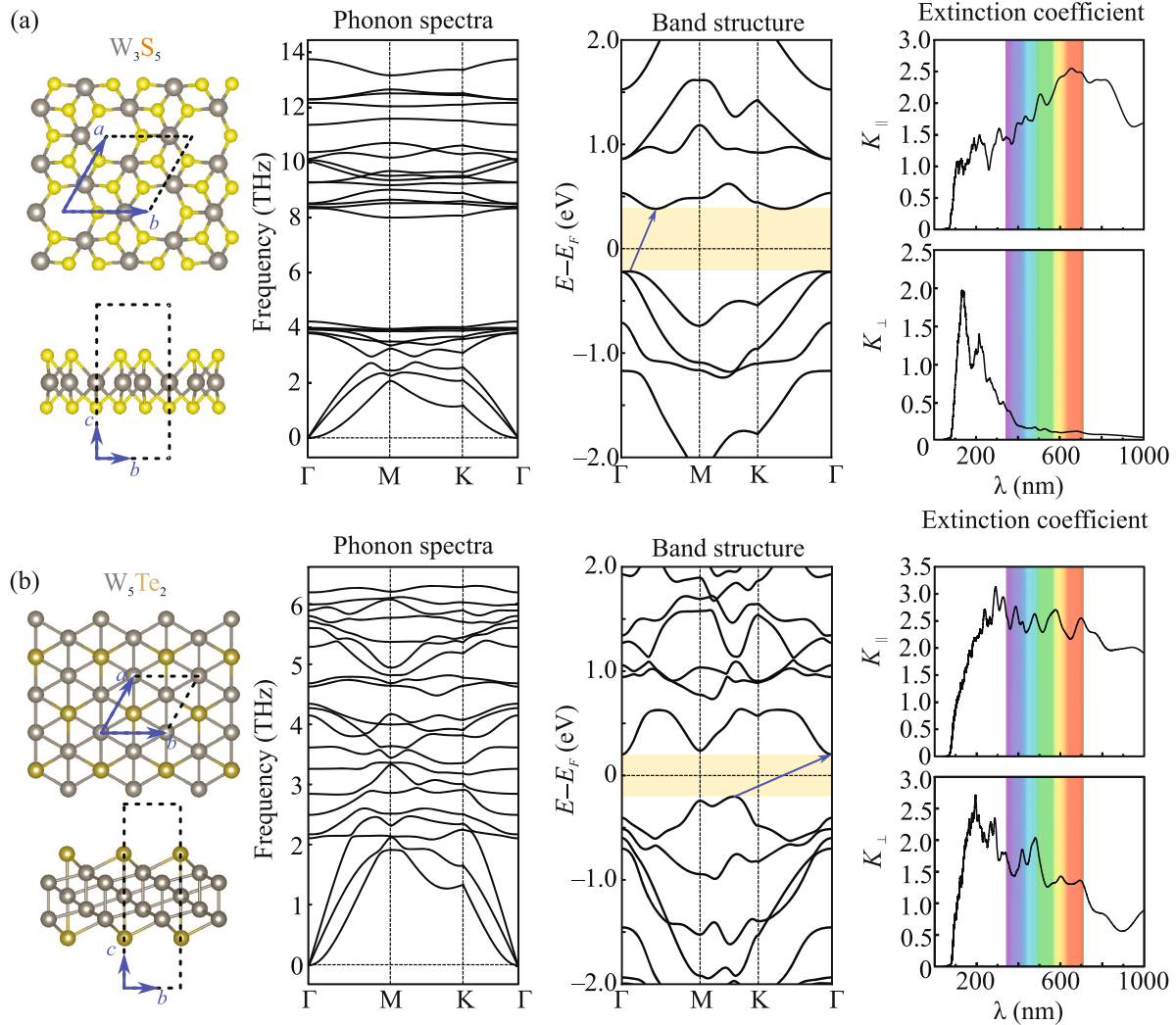


Fig. 2. (Color online) Atomic structure, electronic band structure, spectrum of phonon vibrations, and monolayer extinction coefficient of (a) W_3S_5 and (b) W_5Te_2 . Tungsten, sulfur, and tellurium are given in gray, yellow, and brown, respectively.

layer in the H phase [52] is thermodynamically stable (Fig. 1b). The T and T' phases of WSe_2 are slightly above the convex hull ($\Delta E_{\text{H-T}} = 0.26$ eV/atom and $\Delta E_{\text{H-T'}} = 0.09$ eV/atom). The evolutionary search for new two-dimensional structures in the W–Te system showed the presence of two thermodynamically stable phases, W_5Te_2 and WTe_2 (Fig. 1c). The predicted structure for the WTe_2 monolayer corresponds to the T' phase known in [19–21]. The H and T- WTe_2 phases are above the convex hull ($\Delta E_{\text{H-T}} = 0.03$ eV/atom and $\Delta E_{\text{T-T'}} = 0.22$ eV/atom), which agrees with the data reported in [53].

Thus, two new structures— W_3S_5 and W_5Te_2 —were predicted during the search. The W_3S_5 monolayer is a new compound; its structure can be represented as a defective T'- WS_2 monolayer, where one-third of sulfur atoms are absent on one of the surfaces (Fig. 2a). The

W_5Te_2 structure can be considered as the tungsten-based layer in the bcc packing (typical of a pure metal) terminated on both sides by tellurium atoms. To estimate the dynamic stability of the predicted structures, we calculated the phonon spectra (Fig. 2), where imaginary vibrational frequencies are absent. The analysis of the electronic band structures demonstrated that both structures are indirect-gap semiconductors with band gaps of 0.62 and 0.40 eV for the W_3S_5 and W_5Te_2 monolayers, respectively (Fig. 2). To estimate the prospects for using the predicted structures as elements of optoelectronic devices, the optical properties of W_3S_5 and W_5Te_2 were studied by calculations of the extinction coefficient (Fig. 2). The extinction coefficient makes it possible to estimate the capability of structures to absorb radiation and was calculated in terms of the real and imaginary parts of the

complex dielectric function dependent on the light wavelength $\epsilon(\lambda) = \epsilon_1(\lambda) + i\epsilon_2(\lambda)$:

$$K(\lambda) = \left[\frac{\sqrt{\epsilon_1^2 + \epsilon_2^2} - \epsilon_1}{2} \right]^{1/2}.$$

The longitudinal and transverse components of the permittivity were considered— ϵ_i^{\parallel} (parallel to the monolayer plane) and ϵ_i^{\perp} (perpendicular to the monolayer plane). When the W_3S_5 monolayer was exposed to the radiation polarized perpendicularly to the surface, two absorption maxima (~ 130 and 200 nm) were observed in the ultraviolet spectral range (Fig. 2a). When the incident radiation was polarized in the longitudinal direction to the monolayer surface, the main absorption peak was observed in the visible range (~ 670 nm), and an intense peak was observed in the near infrared spectral range (~ 840 nm). Thus, this structure can be used as a detector for ultraviolet and infrared radiation. When the W_5Te_2 monolayer was exposed to the radiation polarized perpendicularly to the surface, absorption maxima at the wavelengths of ~ 190 and 260 nm are also observed in the ultraviolet spectral range, which indicates the promise of using the W_5Te_2 as an ultraviolet radiation detector. When the incident radiation was polarized in the longitudinal direction to the monolayer surface, the main absorption peak is observed at the border of ultraviolet radiation and the visible spectral range (~ 290 nm), and several intense peaks are observed in the visible spectral range (Fig. 2b). High extinction coefficients in the visible range make it possible to consider these materials as elements of solar energy; in addition, the prospect of synthesizing these structures by removing light elements from known tungsten dichalcogenides by an electron beam was demonstrated using molybdenum selenide monolayers as an example [33] and was discussed in our previous work [26].

4. CONCLUSIONS

The search for new two-dimensional structures in systems of tungsten chalcogenides $W-X$ ($X = S, Se, Te$) has revealed two new thermodynamically stable structures, W_3S_5 and W_5Te_2 . The analysis of the phonon spectra has confirmed the dynamic stability of the predicted structures. The presented two-dimensional layers are indirect-gap semiconductors with band gaps of 0.62 and 0.40 eV, respectively. The calculation of the extinction coefficients has shown that proposed structures are promising as materials for photovoltaic devices capable of absorbing radiation in a wide optical range; in particular, W_5Te_2 and W_3S_5 can be used as ultraviolet radiation detectors, and W_3S_5 can also be a material for infrared radiation detectors.

ACKNOWLEDGMENTS

We are grateful to the Joint Supercomputer Center of the Russian Academy of Sciences and the Information Computer Center of Novosibirsk State University for providing computational resources.

FUNDING

This work was supported jointly by the Russian Foundation for Basic Research and the Committee on Science, Ministry of Education, Science, Sports, and Culture of Armenia (project no. 20-53-05009 (20RF-185)).

CONFLICT OF INTEREST

The authors declare that they have no conflicts of interest.

OPEN ACCESS

This article is licensed under a Creative Commons Attribution 4.0 International License, which permits use, sharing, adaptation, distribution and reproduction in any medium or format, as long as you give appropriate credit to the original author(s) and the source, provide a link to the Creative Commons license, and indicate if changes were made. The images or other third party material in this article are included in the article's Creative Commons license, unless indicated otherwise in a credit line to the material. If material is not included in the article's Creative Commons license and your intended use is not permitted by statutory regulation or exceeds the permitted use, you will need to obtain permission directly from the copyright holder. To view a copy of this license, visit <http://creativecommons.org/licenses/by/4.0/>.

REFERENCES

1. D. G. Kvashnin and L. A. Chernozatonskii, JETP Lett. **105**, 250 (2017).
2. M. M. Glazov and E. L. Ivchenko, JETP Lett. **113**, 7 (2021).
3. M. M. Makhmudian and A. V. Chaplik, JETP Lett. **114**, 545 (2021).
4. M. A. Akmaev, M. V. Kochiev, A. I. Dulebo, M. V. Pugachev, A. Yu. Kuntsevich, and V. V. Belykh, JETP Lett. **112**, 607 (2020).
5. E. V. Sukhanova, Z. I. Popov, and D. G. Kvashnin, JETP Lett. **111**, 627 (2020).
6. P. L. Pekh, P. V. Ratnikov, and A. P. Silin, JETP Lett. **111**, 90 (2020).
7. H. Zeng, G. B. Liu, J. Dai, Y. Yan, B. Zhu, R. He, L. Xie, S. Xu, X. Chen, W. Yao, and X. Cui, Sci. Rep. **3** (1), 1 (2013).
8. W. H. Lin, P. C. Wu, H. Akbari, G. R. Rossman, N. C. Yeh, and H. A. Atwater, Adv. Mater. **34**, 2104863 (2022).
9. K. A. Brekhov, K. A. Grishunin, N. A. Ilyin, A. P. Shestakova, S. D. Lavrov, and E. D. Mishina, Tech. Phys. Lett. **43**, 1112 (2017).

10. Y. You, X. X. Zhang, T. C. Berkelbach, M. S. Hybertsen, D. R. Reichman, and T. F. Heinz, *Nat. Phys.* **11**, 477 (2015).
11. L. Yuan and L. Huang, *Nanoscale* **7**, 7402 (2015).
12. D. Pasquier and O. V. Yazyev, *2D Mater.* **6**, 025015 (2019).
13. H. Terrones, F. López-Urias, and M. Terrones, *Sci. Rep.* **3**, 1549 (2013).
14. W. Chen, X. Xie, J. Zong, T. Chen, D. Lin, F. Yu, S. Jin, L. Zhou, J. Zou, J. Sun, X. Xi, and Y. Zhang, *Sci. Rep.* **9**, 2685 (2019).
15. M. M. Ugeda, A. Pulkin, S. Tang, H. Ryu, Q. Wu, Y. Zhang, D. Wong, Z. Pedramrazi, A. Martin-Recio, Y. Chen, F. Wang, Z.-X. Shen, S.-K. Mo, O. V. Yazyev, and M. F. Crommie, *Nat. Commun.* **9**, 3401 (2019).
16. W. Chen, M. Hu, J. Zong, X. Xie, Q. Meng, F. Yu, L. Wang, W. Ren, A. Chen, G. Liu, X. Xi, F.-S. Li, J. Sun, J. Liu, and Y. Zhang, *Adv. Mater.* **33**, 2004930 (2021).
17. W. Ding, L. Hu, J. Dai, X. Tang, R. Wei, Z. Sheng, C. Liang, D. Shao, W. Song, Q. Liu, M. Chen, X. Zhu, S. Chou, X. Zhu, Q. Chen, Y. Sun, and S. X. Dou, *ACS Nano* **13**, 1694 (2019).
18. Y. Ma, B. Liu, A. Zhang, L. Chen, M. Fathi, C. Shen, A. N. Abbas, M. Ge, M. Mecklenburg, and C. Zhou, *ACS Nano* **9**, 7383 (2015).
19. S.-Y. Xu, Q. Ma, H. Shen, V. Fatemi, S. Wu, T. R. Chang, G. Chang, A. M. M. Valdivia, C.-K. Chan, Q. D. Gibson, J. Zhou, Z. Liu, K. Watanabe, T. Taniguchi, H. Lin, R. J. Cava, L. Fu, N. Gedik, and P. Jarillo-Herrero, *Nat. Phys.* **14**, 900 (2018).
20. S. Wu, V. Fatemi, Q. D. Gibson, K. Watanabe, T. Taniguchi, R. J. Cava, and P. Jarillo-Herrero, *Science* (Washington, DC, U.S.) **359** (6371), 76 (2018).
21. M. N. Ali, J. Xiong, S. Flynn, J. Tao, Q. D. Gibson, L. M. Schoop, and T. Liang, *Nature* (London, U.K.) **514** (7521), 205 (2014).
22. Y. Ma, L. Kou, X. Li, Y. Dai, and T. Heine, *Phys. Rev. B* **93**, 035442 (2016).
23. W. Li, M. Guo, G. Zhang, and Y. W. Zhang, *Phys. Rev. B* **89**, 205402 (2014).
24. Y. Sun, C. Felser, and B. Yan, *Phys. Rev. B* **92**, 165421 (2015).
25. Z. Chen and L.-W. Wang, *Chem. Mater.* **30**, 6242 (2018).
26. T. Joseph, M. Ghorbani-Asl, A. G. Kvashnin, K. V. Laktionov, Z. I. Popov, P. B. Sorokin, and A. V. Krasheninnikov, *J. Phys. Chem. Lett.* **10**, 6492 (2019).
27. Z. Zhou, T. Xu, C. Zhang, S. Li, J. Xu, L. Sun, and L. Gao, *Nano Res.* **14**, 1704 (2021).
28. J. Zhang, Y. Xia, B. Wang, Y. Jin, H. Tian, W. kin Ho, H. Xu, C. Jin, and M. Xie, *2D Mater.* **8**, 015006 (2020).
29. J. C. Kotsakidis, Q. Zhang, A. L. Vazquez de Parga, M. Currie, K. Helmerson, D. K. Gaskill, and M. S. Fuhrer, *Nano Lett.* **19**, 5205 (2019).
30. L. Ma, Y. Tan, M. Ghorbani-Asl, R. Boettger, S. Kretschmer, S. Zhou, Z. Huang, A. V. Krasheninnikov, and F. Chen, *Nanoscale* **9**, 11027 (2017).
31. B. Huang, F. Tian, Y. Shen, M. Zheng, Y. Zhao, J. Wu, Y. Liu, S. J. Pennycook, and J. T. Thong, *ACS Appl. Mater. Interfaces* **11**, 24404 (2019).
32. X. Wang, X. Guan, X. Ren, T. Liu, W. Huang, J. Cao, and C. Jin, *Nanoscale* **12**, 8285 (2020).
33. X. Zhao, J. Dan, J. Chen, Z. Ding, W. Zhou, K. P. Loh, and S. J. Pennycook, *Adv. Mater.* **30**, 1707281 (2018).
34. A. R. Oganov and C. W. Glass, *J. Chem. Phys.* **124**, 244704 (2006).
35. A. R. Oganov, Y. Ma, A. O. Lyakhov, M. Valle, and C. Gatti, *Rev. Miner. Geochem.* **71**, 271 (2010).
36. A. R. Oganov, A. O. Lyakhov, and M. Valle, *Acc. Chem. Res.* **44**, 227 (2011).
37. A. O. Lyakhov, A. R. Oganov, H. T. Stokes, and Q. Zhu, *Comput. Phys. Commun.* **184**, 1172 (2013).
38. P. V. Bushlanov, V. A. Blatov, and A. R. Oganov, *Comput. Phys. Commun.* **236**, 1 (2019).
39. P. Hohenberg and W. Kohn, *Phys. Rev. B* **136**, 864 (1964).
40. W. Kohn and L. J. Sham, *Phys. Rev. A* **140**, 1133 (1965).
41. J. P. Perdew and K. Burke, *Phys. Rev. Lett.* **77**, 3865 (1996).
42. G. Kresse and J. Hafner, *Phys. Rev. B* **47**, 558 (1993).
43. G. Kresse and J. Hafner, *Phys. Rev. B* **49**, 14251 (1994).
44. G. Kresse and J. Furthmüller, *Phys. Rev. B* **54**, 11169 (1996).
45. H. J. Monkhorst and J. D. Pack, *Phys. Rev. B* **13**, 5188 (1976).
46. A. Togo and I. Tanaka, *Scr. Mater.* **108**, 1 (2015).
47. A. Togo, F. Oba, and I. Tanaka, *Phys. Rev. B* **78**, 134106 (2008).
48. A. S. Nissimagoudar, A. Manjanath, and A. Singh, *Phys. Chem. Chem. Phys.* **18**, 14257 (2016).
49. Y. D. Kuang, L. Lindsay, S. Q. Shi, and G. P. Zheng, *Nanoscale* **8**, 3760 (2016).
50. F. Eriksson, E. Fransson, and P. Erhart, *Adv. Theory Simul.* **2**, 1800184 (2019).
51. M. Gajdos, K. Hummer, G. Kresse, J. Furthmüller, and F. Bechstedt, *Phys. Rev. B* **73**, 045112 (2006).
52. C. Ataca, H. Sahin, and S. Ciraci, *J. Phys. Chem. C* **116**, 8983 (2012).
53. H. H. Huang, X. Fan, D. J. Singh, H. Chen, Q. Jiang, and W. T. Zheng, *Phys. Chem. Chem. Phys.* **18**, 4086 (2016).

Translated by R. Bando